

## Magnetization-dependent behaviors of interband transitions between the exchange-split bands in doped manganite films

Y. Moritomo, A. Machida, K. Matsuda, M. Ichida, and A. Nakamura

Center for Integrated Research in Science and Engineering (CIRSE) and Department of Applied Physics, Nagoya University,  
Nagoya 464-01, Japan

(Received 11 March 1997)

The temperature dependence of absorption spectra for thin films of double-exchange ferromagnet  $R_{0.6}\text{Sr}_{0.4}\text{MnO}_3$  has been investigated with variation of the one-electron bandwidth  $W$ . With decreasing temperature, which corresponds to the increase of the magnetization  $M$ , a large amount of spectral weight transfers from the high- ( $\sim 3$  eV) to low- ( $\leq 1$  eV) energy region. We ascribe these transitions to the interband transition between the bands split by the on-site exchange interaction  $J$  and the intraband transition within the lower band, respectively. This suggests that optical excitations in the visible region strongly couple with local spin alignments in these doped manganites. [S0163-1829(97)01733-5]

The conducting ferromagnetic state in the hole-doped manganese oxides with perovskite structure, e.g.,  $\text{La}_{1-x}\text{Sr}_x\text{MnO}_3$ , is mediated by the double-exchange (DE) interaction.<sup>1-4</sup> Recent extensive investigations on the electronic properties have revealed colossal magnetoresistance (MR) phenomena<sup>5-7</sup> near the ferromagnetic transition temperature  $T_C$ , which is attracting broad interest from the viewpoint of applications. The generic magnetic and transport properties in the doped manganites mainly arise from a strong on-site exchange interaction (Hund's-rule coupling  $J \sim 2$  eV) between the localized  $t_{2g}$  spins and itinerant  $e_g$  electrons. The one-electron bandwidth  $W$  of the  $e_g$  state is likely to be smaller than  $J$  in these doped manganites, and hence the  $e_g$  carriers in the ferromagnetic ground state are almost perfectly spin polarized, in contrast to the case of conventional itinerant ferromagnets. The MR behavior especially for  $\text{La}_{1-x}\text{Sr}_x\text{MnO}_3$  Ref. (4) having maximal  $W$  is well accounted for by a simple DE model<sup>3</sup> that includes only the transfer integral  $t$  of the  $e_g$  electrons and  $J$ . In these systems with a large  $J$  value corresponding to the photon energy in the visible region, one can expect that there appears strong coupling of the optical excitations with the  $t_{2g}$ -spin alignment, and such a feature affects significantly the optical spectrum. Recently, several researchers have reported a significant variation of the optical spectra for doped manganites, e.g.,  $\text{La}_{0.825}\text{Sr}_{0.175}\text{MnO}_3$  crystal<sup>8</sup> and  $\text{Nd}_{0.7}\text{Sr}_{0.3}\text{MnO}_3$  film.<sup>9</sup> However, there exists a large discrepancy between the spectral behaviors reported in the literature probably due to the different doping level  $x$ . In addition, the investigations are restricted in the narrow energy regions below  $\sim 2$  eV Ref. (8) or  $\sim 3$  eV Ref. (9), even though their results imply that the spectral change extends far above 3 eV.

In this paper, we report on the temperature variation of optical spectrum in the energy range of 0.5–5 eV for thin films of  $R_{0.6}\text{Sr}_{0.4}\text{MnO}_3$  ( $R = \text{La}, \text{La}_{1/2}\text{Nd}_{1/2}, \text{Nd}_{1/2}\text{Sm}_{1/2},$  and  $\text{Sm}$ ) with a fixed hole concentration of  $x=0.4$ . The  $W$  value was controlled by changing the trivalent rare-earth ions, because  $W$  depends on the average ionic radius  $r_A$  of the perovskite  $A$  site.<sup>10</sup> We observed a large transfer of spectral weight from the high- ( $\sim 3$  eV) to low- ( $\leq 1$  eV) energy

region with decreasing temperature, equivalently corresponding to increasing magnetization  $M$ . These observations are well interpreted in terms of the transfer of spectral weight from the interband transitions between the exchange-split  $e_g$  bands to the intraband transitions within the lower band. The findings indicate that the local  $t_{2g}$ -spin alignment affects not only the transport properties but also optical transitions in the visible (2–4 eV) regions.

Thin films of  $R_{0.6}\text{Sr}_{0.4}\text{MnO}_3$  ( $R = \text{La}, \text{La}_{0.5}\text{Nd}_{0.5}, \text{Nd}_{0.5}\text{Sm}_{0.5},$  and  $\text{Sm}$ ) with thickness of  $\sim 100$  nm were fabricated using a vacuum pulsed-laser deposition (PLD) apparatus. Calcined powder was pressed into a pellet with a size of 20 mm  $\times$  5 mm and sintered at 1300 °C for 48 h. An excimer laser beam of 248 nm with a repetition rate of  $\approx 5$  Hz and pulse energy of  $\approx 80$  mJ was focused onto the target in the vacuum chamber. The compound was deposited on to a MgO (100) substrate that was heated at 850–950 °C in an atmosphere of  $\approx 300$  mTorr oxygen. The MgO substrate is transparent in a wide energy region of 0.1–5.0 eV, and is suitable for the optical measurements. The fabricated films were annealed in 760 Torr oxygen atmosphere for 1 h, and then slowly cooled down. X-ray-diffraction measurements revealed that the obtained films were (110) oriented in the pseudocubic setting. The thicknesses of the films were measured by a scanning electron microscope (SEM). An absorption coefficient  $\alpha(\omega)$  was determined from transmission spectra using the standard formula, neglecting a multiple-reflection effect, since the optical density of our films is larger than 0.7 in the spectral region investigated.

We show in Fig. 1 temperature dependence of magnetization  $M$  for thin films of doped manganites with systematic variation of  $r_A$ , that is,  $W$ .  $M$  was measured under a field of 0.5 T after cooling down to 5 K in zero field (ZFC).  $T_C$  was determined from the inflection point of the  $M$ - $T$  curve. In  $\text{La}_{0.6}\text{Sr}_{0.4}\text{MnO}_3$  which has maximal  $W$ , magnetization begins to rise below  $T_C \approx 325$  K (indicated by a downward arrow). With decreasing  $r_A$ ,  $T_C$  decreases down to  $\approx 175$  K for  $R = \text{Nd}_{0.5}\text{Sm}_{0.5}$ , and eventually the transition disappears for  $R = \text{Sm}$  (see also the inset of Fig. 1). The observed critical temperatures are consistent with the previously reported ones

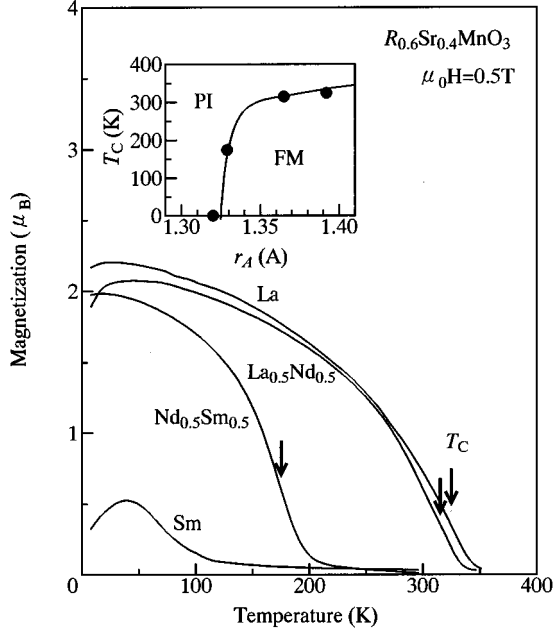


FIG. 1. Temperature dependence of magnetization for thin films of  $R_{0.6}\text{Sr}_{0.4}\text{MnO}_3$ . Magnetization was measured in a field of 0.5 T after cooling down to 5 K in the zero field (ZFC). Vertical arrows represent the Curie temperatures  $T_C$ . Inset represents relation between  $T_C$  and average ionic radius  $r_A$  of the perovskite A site. FM and PI represent ferromagnetic metallic and paramagnetic insulating phases, respectively.

for thin films.<sup>11</sup> To check the quality of these thin films, we further measured resistivities  $\rho$  up to  $\sim 400$  K (not shown). For  $R=\text{La}$ ,  $\text{La}_{0.5}\text{Nd}_{0.5}$ , and  $\text{Nd}_{0.5}\text{Sm}_{0.5}$ , the  $\rho$ - $T$  curve gradually increases with decreasing temperature above  $T_C$  and then decreases below  $T_C$ , similarly to the case of the melt-grown crystals.<sup>4</sup> In  $\text{La}_{0.6}\text{Sr}_{0.4}\text{MnO}_3$ , especially, the  $\rho$  value becomes sufficiently low ( $< 1 \times 10^{-3} \Omega \text{ cm}$ ) in the ferromagnetic phase, indicating a high quality of our thin films. In the case of  $\text{Sm}_{0.6}\text{Sr}_{0.4}\text{MnO}_3$  having minimal  $W$ , however, resistivity remains insulating down to the lowest temperature in this study.

Figure 2 shows variation of the absorption spectrum  $\alpha(\omega)$  in the temperature range of 6–400 K for  $\text{La}_{0.6}\text{Sr}_{0.4}\text{MnO}_3$  ( $T_C \approx 325$  K). The thick solid (dashed) curve represents the spectrum of the lowest (highest) temperature. With decreasing temperature, the spectral shape significantly changes in the wide energy range of 0.5–4.0 eV. Similar behaviors are observed in the spectra for  $R=\text{La}_{0.5}\text{Nd}_{0.5}$  ( $T_C \approx 315$  K) and  $\text{Nd}_{0.5}\text{Sm}_{0.5}$  ( $T_C \approx 175$  K). In  $\text{Sm}_{0.6}\text{Sr}_{0.4}\text{MnO}_3$  where the ferromagnetic transition does not appear, the behavior is qualitatively different: The spectral weight below  $\sim 1.0$  eV transfers to the higher-energy region with decreasing temperature, showing a gap-opening behavior. To analyze the spectral behavior more in detail, let us decompose  $\alpha(\omega)$  into temperature-dependent [ $\alpha_T(\omega)$ ] and temperature-independent [ $\alpha_0(\omega)$ ] (the hatched region of the spectrum in Fig. 2) components as

$$\alpha(\omega) = \alpha_T(\omega) + \alpha_0(\omega). \quad (1)$$

The  $\alpha_0(\omega)$  component is considered to be dominated by the charge-transfer (CT) transitions from the ligand  $p$  states to

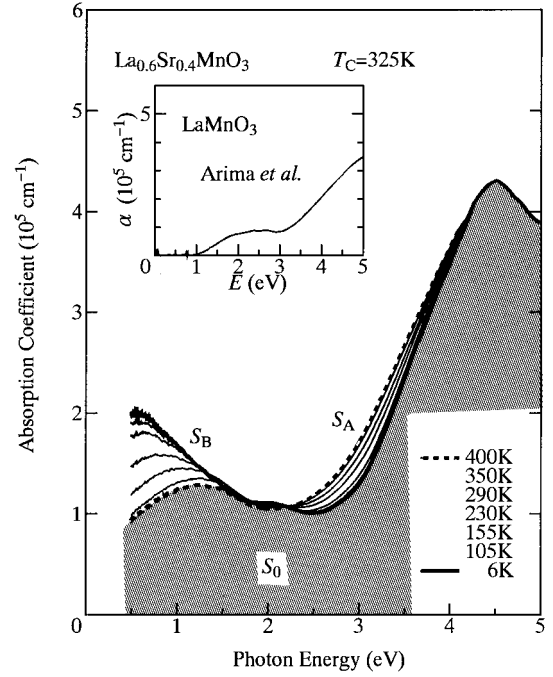


FIG. 2. Temperature dependence of absorption spectrum  $\alpha(\omega)$  for  $\text{La}_{0.6}\text{Sr}_{0.4}\text{MnO}_3$  film. The hatched area represents the temperature-independent component  $\alpha_0(\omega)$ . Inset shows the  $\alpha(\omega)$  spectrum for the parent  $\text{LaMnO}_3$  crystal.

the Mn  $3d$  levels. In the inset of Fig. 2, we show the  $\alpha(\omega)$  spectrum for a single crystal of  $\text{LaMnO}_3$  (cited from Arima *et al.*<sup>12</sup>). In the energy region below  $\sim 5$  eV, the spectrum consists of two CT-type transitions around  $\sim 2$  eV and  $\sim 4$  eV. The former and the latter correspond to the CT transitions of an up-spin and a down-spin electron, respectively.<sup>12,13</sup> Corresponding structures are observed for the  $\alpha_0(\omega)$  spectrum around  $\sim 1.3$  eV and  $\sim 4$  eV. Note that the energy splitting of these transitions is of the order of  $J$ .

Now, let us proceed to the temperature-dependent component  $\alpha_T(\omega)$ . With decreasing temperature, i.e., from the broken spectrum to the solid one, the spectral weight decreases in the energy region of 2.2–4.0 eV, while it increases below 2.2 eV. Hereafter, we define the areas, i.e.,  $S_A$ ,  $S_B$ , and  $S_0$ , of the higher- and lower-lying spectral regions of  $\alpha_T(\omega)$  and  $\alpha_0(\omega)$  as

$$S_A \equiv \int_{2.2 \text{ eV}}^{4.0 \text{ eV}} \alpha_T(\omega) d\omega, \quad (2)$$

$$S_B \equiv \int_{0.5 \text{ eV}}^{2.2 \text{ eV}} \alpha_T(\omega) d\omega, \quad (3)$$

and

$$S_0 \equiv \int_{0.5 \text{ eV}}^{4.0 \text{ eV}} \alpha_0(\omega) d\omega. \quad (4)$$

As discussed above, the spectral weight  $S_0$  originates from the CT-type transitions. We plotted in Fig. 3 the relative magnitudes of the higher- and lower-lying components for thin films of  $R_{0.6}\text{Sr}_{0.4}\text{MnO}_3$  as a function of temperature. In the case of  $(\text{Nd}_{0.5}\text{Sm}_{0.5})_{0.6}\text{Sr}_{0.4}\text{MnO}_3$ , the relative magni-

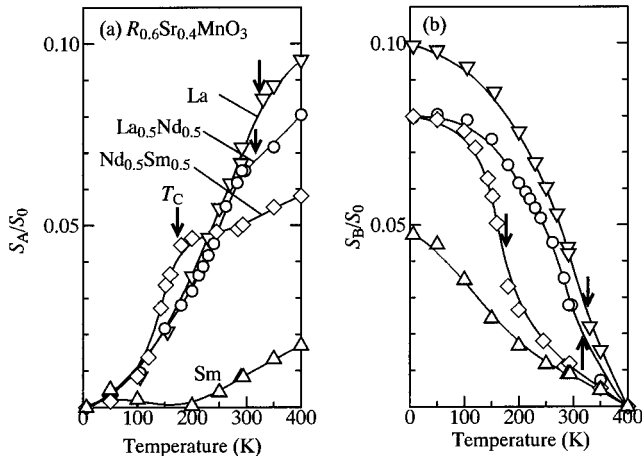


FIG. 3. Temperature dependence of spectral weights of (a) the higher-lying component [ $S_A \equiv \int_{2.2 \text{ eV}}^{4.0 \text{ eV}} \alpha_T(\omega) d\omega$ ] and (b) the lower-lying component [ $S_B \equiv \int_{0.5 \text{ eV}}^{2.2 \text{ eV}} \alpha_T(\omega) d\omega$ ] for thin films of  $R_{0.6}\text{Sr}_{0.4}\text{MnO}_3$ . The spectral weight is normalized by that of the temperature-independent component [ $S_0 \equiv \int_{0.5 \text{ eV}}^{4.0 \text{ eV}} \alpha_0(\omega) d\omega$ ]. Arrows represent the Curie temperatures.

tude of the A component  $S_A/S_0$  exhibits a weak temperature variation above  $T_C \approx 175$  K (indicated by a downward arrow), but steeply decreases below  $T_C$  [see Fig. 3(a)]. A similar behavior is also observed for  $R=\text{La}$  and  $\text{La}_{0.5}\text{Nd}_{0.5}$ , as indicated by an arrow. In the insulating  $\text{Sm}_{0.6}\text{Sr}_{0.4}\text{MnO}_3$ , however,  $S_A/S_0$  does not show any prominent temperature dependence. As seen in Fig. 3(b), the lost spectral weight of the A component is transferred into the lower-lying B component. For example,  $S_B/S_0$  for  $(\text{Nd}_{0.5}\text{Sm}_{0.5})_{0.6}\text{Sr}_{0.4}\text{MnO}_3$  steeply increases below  $T_C$  (downward arrow), which almost complements the decrease of  $S_A/S_0$ . In the wider- $W$  (high- $T_C$ ) compounds, the rise of  $S_B/S_0$  shifts toward the higher-temperature side. Thus, the spectral change, being apparently temperature dependent, is governed by the spin polarization. This argument is consistent with effects of an external magnetic field on the optical spectrum for  $\text{Nd}_{0.7}\text{Sr}_{0.3}\text{MnO}_3$  reported by Kaplan *et al.*:<sup>9</sup> They found that the spectral change under the magnetic field is similar to the temperature variation of the spectrum.

The A and B components, whose spectral intensities are strongly dependent on the spin polarization, can be interpreted in the following way. The strong on-site exchange interaction [ $J \sim 2$  eV (Refs. 12 and 13)] between the  $e_g$  electron and the  $t_{2g}$  spins ( $S=3/2$ ) exceeds  $W$ , and hence the  $e_g$  band should be split into two bands by  $\sim J$ .<sup>8</sup> Note that optical transitions are allowed only between the same spin species. We show in the inset of Fig. 4 the schematic energy structures of the exchange-split  $e_g$  states with up spins ( $\uparrow$ ) and down spins ( $\downarrow$ ) for the ferromagnetic phase ( $T < T_C$ , left figure) and the paramagnetic phase ( $T > T_C$ , right figure). In the paramagnetic phase, the occupation of the up-spin  $e_g$  state (or the down-spin  $e_g$  state) is the same in both the bands, and hence the interband transitions between the  $J$ -split bands occur strongly. The higher-lying A component observed above  $T_C$  is assigned to such an interband transition, while the lower-lying B component is assigned to the intraband transition within the lower band. In the case of the

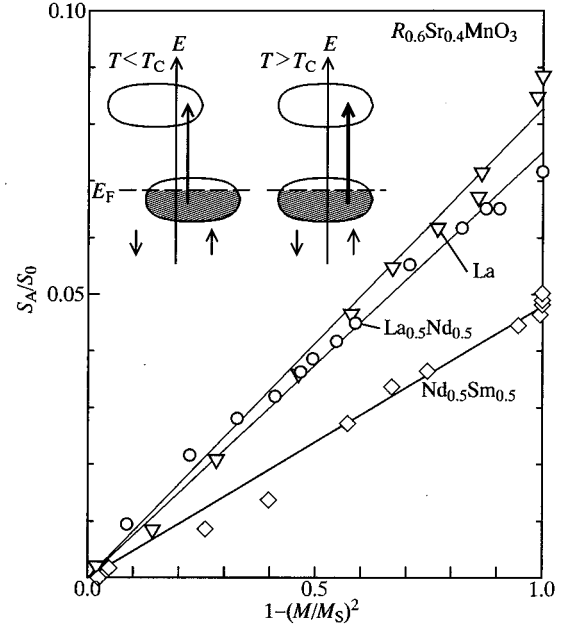


FIG. 4. The relative intensity of the interband transition ( $S_A/S_0$ ) vs  $1 - (M/M_s)^2$  for thin films of  $R_{0.6}\text{Sr}_{0.4}\text{MnO}_3$ . The inset depicts the schematic band structures of the exchange-split  $e_g$  states with up spins ( $\uparrow$ ) and down spins ( $\downarrow$ ).

$R_{0.6}\text{Sr}_{0.4}\text{MnO}_3$ , the interband transition locates at  $E_{\text{gap}} \approx 3.0$  eV.

With decreasing temperature below  $T_C$ , the induced magnetization significantly modifies the occupations of the up- and down-spin states in both the  $J$ -split bands, as shown in the inset of Fig. 4. In the strong-coupling limit ( $J \gg W$ ), the spectral weight of the interband transition (indicated by upward arrows) decreases with the spin polarization  $M/M_s$  as  $\propto 1 - (M/M_s)^2$ . We plot in Fig. 4 the relative magnitude of  $S_A/S_0$  for thin films of  $R_{0.6}\text{Sr}_{0.4}\text{MnO}_3$  as a function of  $1 - (M/M_s)^2$ . The values of  $M$  were estimated under a field of 0.5 T to avoid the complexity arising from the nonremanent behavior of the present system.<sup>4</sup> The change of the spectral weight ( $S_A/S_0$ ) with temperature is well reproduced by the temperature-dependent spin polarization, indicating that the component should be characterized as the interband transitions. On the other hand, the modified occupations enhance the intraband excitation within the lower band, which corresponds to the growth of the Drude-like B component at low temperatures [see Fig. 3(b)]. The spectral weight of the intraband transition increases approximately in proportion to  $M/M_s$ , which differs from the expected  $(M/M_s)^2$  dependence. This suggests that additional interactions, such as the Jahn-Teller (JT) coupling<sup>14</sup> or the orbital fluctuation,<sup>15</sup> dominate the low-energy intraband transitions as well as the transport properties. Okimoto *et al.*<sup>8</sup> have observed similar temperature-sensitive excitations below  $\sim 1$  eV for  $\text{La}_{0.825}\text{Sr}_{0.175}\text{MnO}_3$  crystal, in which the temperature dependence is not expressed by  $M/M_s$  or  $(M/M_s)^2$ .

Finally, let us discuss the strength of the interband transition between the  $J$ -split bands. As seen in Fig. 4, the relative magnitude  $S_A/S_0$  of the interband transitions at  $M/M_s \approx 0$  (high-temperature limit) is strongly material dependent, and increases from  $\approx 0.05$  for  $R=\text{Nd}_{0.5}\text{Sm}_{0.5}$  to  $\approx 0.08$  for

$R=\text{La}$ . This enhancement can be ascribed to the variation of the corresponding transition matrix element between the neighboring  $e_g$  orbitals. The matrix element increases with the transfer integral  $t$ , and  $t$  increases when we change the material from  $R=\text{Nd}_{0.5}\text{Sm}_{0.5}$  to La. Thus, the strength of the interband transitions in the optical spectrum reflects the magnitude of  $W$ .

In conclusion, we have investigated the strongly temperature-dependent behaviors of the optical spectra up to  $\sim 5$  eV for doped manganites with variation of the  $W$  value. We have observed two characteristic optical transitions around  $\sim 3$  eV and  $\sim 1$  eV, and ascribed them to the interband and intraband transitions of the exchange-split bands. The temperature dependence of the interband transitions is well explained by that of  $1 - (M/M_s)^2$ , as is expected from a mean-field-type interpretation. Thus, in the doped mangan-

ites, the strong on-site exchange interaction  $J$  governs not only the magnetic and electronic properties but also the optical excitations in the visible region. The strong coupling of the optical excitations with the  $t_{2g}$ -spin alignment suggests a controllability of the spin system by means of irradiation of visible light, which may lead us to apply the system to magneto-optical devices with a photon mode. A study along this trend is now in progress and will be published in a separate paper.

We thank N. Furukawa for fruitful discussions. We are also indebted to T. Sumi for building the pulsed-laser deposition (PLD) chamber used in this study. This work was supported by a Grant-In-Aid for Scientific Research from the Ministry of Education, Science and Culture, Japan and also from Murata Science Foundation.

<sup>1</sup>P. W. Anderson and H. Hasagawa, Phys. Rev. **100**, 675 (1955).

<sup>2</sup>P. -G. de Gennes, Phys. Rev. **118**, 141 (1960).

<sup>3</sup>N. Furukawa, J. Phys. Soc. Jpn. **63**, 3214 (1994); **64**, 2734 (1995); **64**, 2754 (1995); **64**, 3164 (1995).

<sup>4</sup>A. Urushibara, Y. Moritomo, T. Arima, A. Asamitsu, G. Kido, and Y. Tokura, Phys. Rev. B **51**, 14 103 (1995); Y. Tokura, A. Urushibara, Y. Moritomo, T. Arima, A. Asamitsu, and G. Kido, J. Phys. Soc. Jpn. B **63**, 3931 (1994).

<sup>5</sup>K. Chahara, T. Ohno, M. Kasai, and Y. Kozono, Appl. Phys. Lett. **63**, 1990 (1993).

<sup>6</sup>R. von Helmolt, J. Wecker, B. Holzapfel, L. Schultz, and K. Samwer, Phys. Rev. Lett. **71**, 2331 (1993).

<sup>7</sup>S. Jin, T. H. Tiefel, M. McCormack, R. Fastnacht, R. Ramesh, and L. H. Chen, Science **264**, 13 (1994).

<sup>8</sup>Y. Okimoto, T. Katsufuji, T. Ishikawa, A. Urushibara, T. Arima, and Y. Tokura, Phys. Rev. Lett. **75**, 109 (1996).

<sup>9</sup>S. G. Kaplan, M. Quijada, H. D. Drew, D. B. Tanner, G. C. Xiong, R. Ramesh, C. Kwon, and T. Venkatesan, Phys. Rev. Lett. **77**, 2081 (1996).

<sup>10</sup>H. Y. Hwang, S. -W. Cheong, P. G. Radaelli, M. Marezio, and B. Batlogg, Phys. Rev. Lett. **75**, 914 (1995).

<sup>11</sup>For example, M. Kasai, H. Kuwahara, Y. Moritomo, Y. Tomioka, and Y. Tokura, Jpn. J. Appl. Phys. **35**, L489 (1996).

<sup>12</sup>T. Arima, Y. Tokura, and J. B. Torrance, Phys. Rev. B **48**, 17 006 (1993); T. Arima and Y. Tokura, J. Phys. Soc. Jpn. **64**, 2488 (1995).

<sup>13</sup>Y. Moritomo, T. Arima, and Y. Tokura, J. Phys. Soc. Jpn. **64**, 4117 (1995).

<sup>14</sup>A. J. Millis, P. B. Littlewood, and B. I. Shraiman, Phys. Rev. Lett. **74**, 5144 (1994); **77**, 175 (1996).

<sup>15</sup>S. Ishihara, M. Yamanaka, and N. Nagaosa, Phys. Rev. B (to be published).